

A Simple Electronic Circuit Realization of the Tent Map

I. CAMPOS-CANTÓN¹, E. CAMPOS-CANTÓN², J. S. MURGUÍA² AND H. C. ROSU³

¹FAC. DE CIENCIAS, ²DEPARTAMENTO DE FÍSICO MATEMÁTICAS,
Universidad Autónoma de San Luis Potosí,
Alvaro Obregón 64, 78000, San Luis Potosí, SLP, México

³DIVISIÓN DE MATERIALES AVANZADOS,
Instituto Potosino de Investigación Científica y Tecnológica
Camino a la presa San José 2055, 78216, San Luis Potosí, SLP, México

ICAMPOS@GALIA.FC.UASLP.MX, ECAMP@UASLP.MX, ONDELETO@UASLP.MX, HCR@IPICYT.EDU.MX

Abstract

We present a very simple electronic implementation of the tent map, one of the best-known discrete dynamical systems. This is achieved by using integrated circuits and passive elements only. The experimental behavior of the tent map electronic circuit is compared with its numerical simulation counterpart. We find that the electronic circuit presents fixed points, periodicity, period doubling, chaos and intermittency that match with high accuracy the corresponding theoretical values.

PACS:84.30.-r; 05.45.-a; 02.30.Oz

KEYWORDS: Electronic circuits, nonlinear dynamics and chaos, bifurcation theory.

TMap-fin1.tex
 arXiv: 0807.3375

Chaos, Solitons & Fractals 42 (2009) 12–16

1 Introduction

Discrete-time nonlinear dynamical systems are generally described as iterative maps $f : \mathfrak{R}^k \rightarrow \mathfrak{R}^k$ given by their state equation

$$\mathbf{x}_{n+1} = f(\mathbf{x}_n), \quad n = 0, 1, 2, \dots, \quad (1)$$

where \mathbf{x}_0 is the initial state, k is the dimensionality of the state space, $\mathbf{x}_n \in \mathfrak{R}^k$ is the state of the system at time n , and \mathbf{x}_{n+1} denotes the next state. The interpretation of the state vector depends on the context. For example, in population biology \mathbf{x}_n is usually the population size in generation n , in epidemiology it is the fraction of the population infected at time n , whereas in economics it can be the price per unit at time n for a certain commercial product. Repeated iteration of f gives a sequence of points $\{\mathbf{x}_n\}_{n=0}^{\infty}$ that is known as an orbit. Clearly, equation (1) is a difference equation. In the words of R.M. May [1], *such equations, even though simple and deterministic, can exhibit a surprising array of dynamical behaviour, from stable points, to a bifurcating hierarchy of stable cycles, to apparently random fluctuations.* The tent map is one of the simplest iterated functions and, either alone or in more general forms, has been the subject of interesting papers published in this journal, see e.g., [2, 3, 4]. It has the shape of a tent as is shown in Fig. 1. It takes a point x_n on the real line and maps it to another point given by the following equation

$$x_{n+1} = \begin{cases} \mu x_n & \text{for } x_n < \frac{1}{2} \\ \mu(1 - x_n) & \text{for } \frac{1}{2} \leq x_n, \end{cases} \quad (2)$$

where $x_n \in [0, 1]$, and $\mu \in [1, 2]$ is a bifurcation parameter that controls the properties of the tent map. Many of the basic properties of the tent map can be found in the book of Elaydi [5] on discrete chaos.

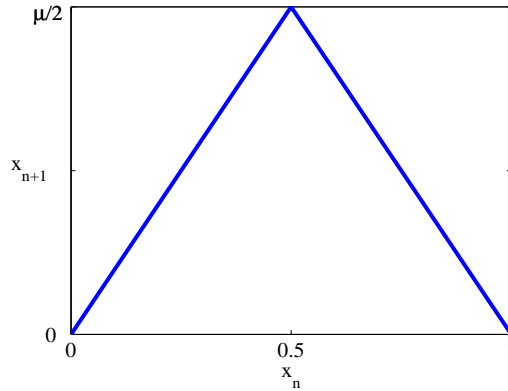


Fig. 1: Plot of the tent map function.

The tent map is a very simple model for studying a variety of nonlinear phenomena. The nonlinear dynamics of the tent map has found applications in as different areas as biophysics, meteorology, hydrodynamics, chemical engineering, optics, cryptology, and communications. For example, in [6] the tent map is used to illustrate the synchronization and/or non-synchronization of chaos, which raised considerable interest in finding simple circuits that exhibit nonlinear phenomena. Murali *et al* [7] provided a proof of principle experiment of the capability of chaotic systems for universal computing.

In general, any map can be electronically designed. Following Tanaka *et al.* [8], a typical circuit diagram of a chaotic one-dimensional map with its iterative operation is shown in Fig. 2. In this paper, we present one of the simplest electronic implementation of the tent map, which at the same time is a good engineering model of the corresponding mathematical system. Through the variation of the tent map control parameter μ , one can examine the bifurcation diagram of the realized system and we were able to reproduce the theoretical diagram with high accuracy.

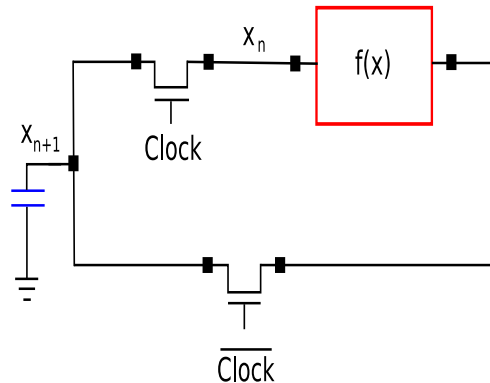


Fig. 2: A typical block diagram of a map.

2 Electronic implementation of the tent map

In several implementations of this kind of circuits [9, 10] analog multipliers have been employed with a normalization of the signal by a factor of about ten. This normalization was necessary because of the physical restrictions in the analog multiplier. The starting point is a block diagram of the tent map that is shown in Fig. 3. Typically, these circuits contain several operational amplifiers, which perform linear operations (e.g., integration and summation), as well as a couple of integrated circuits that perform the nonlinear operations (i.e., multiplication). In general, a large number of active components make it difficult to directly extrapolate these designs to high frequencies. Another approach is to use a digital signal processor and digital-to-analog converters. Here, we describe a new circuit that contains active components, speeds of

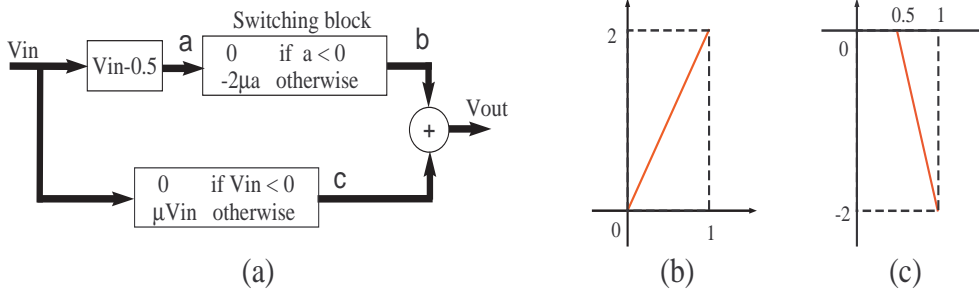


Fig. 3: (a) Block diagram of the tent map used to construct the electronic circuit. (b) Response of the lower branch of the block diagram. (c) Response of the upper branch of the block diagram.

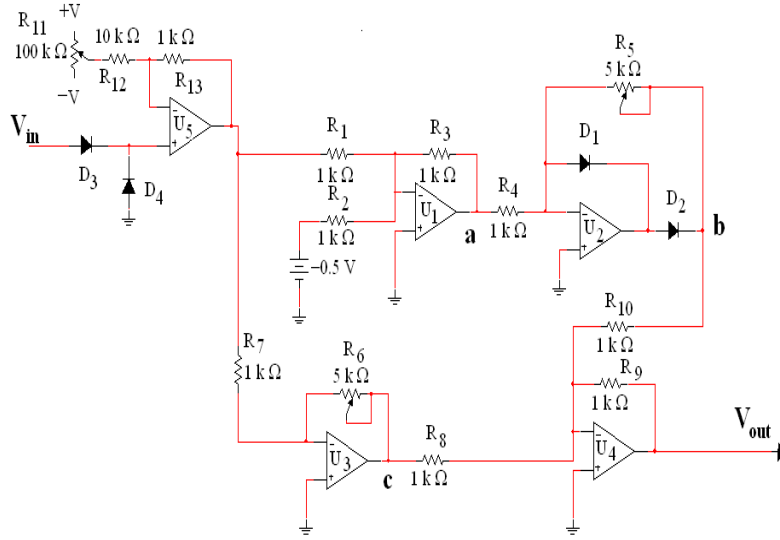


Fig. 4: Schematic diagram of the tent map electronic circuit.

radio frequencies, and capable of reproducing the transition from steady state to chaos as observed in the tent map equation when the bifurcation parameter is varied.

We now introduce a designed circuit of the tent map based on Fig. 3. The flow diagram of the tent map used to construct the electronic circuit is shown in Fig. 3 (a). The behavior of the tent map is based on two straight lines given by $l_1 : \mu V_{in}$ and $l_2 : -2\mu V_{in} + 1$ with domains $[0, \infty)$ and $[0.5, \infty)$, respectively. The output V_{out} is given by l_1 when V_{in} belongs to the interval $[0V, 0.5V)$ and by $l_1 + l_2$ when V_{in} is in the interval $[0.5V, 1V)$. The responses of the lower and upper branches are shown in Figs. 3 (b) and (c), respectively. This simple approach allows for the changing of the slope from μ to $-\mu$. One can think of the system as having two weak points, $V_{in} < 0$ and $V_{in} > 1$. However, the response of the circuit is zero for these inputs. In the absence of noise the tent map circuit can remain in one of the fixed points, but in the real world of analog electronic components there always exists some noise that generates the dynamics in the circuit. The schematic diagram of the tent map circuit is shown in Fig. 4, which consists of five operational amplifiers (from U_1 to U_5), four diodes ($D_1 - D_4$), thirteen resistors (from R_1 to R_{13}), and a dc voltage source (Vdc). The simplicity of this circuit is due to the fact that the linear mathematical operation of commutation is performed by the operational amplifiers in the switching block, as is shown in Fig. 3.

Assuming ideal performance from all components, the circuit in Fig. 4 is modeled by the following equation

Device	Value
$R_{1,2,3,4,7,8,9,10,12,13}$	1 k Ω resistor
$R_{5,6}$	5 k Ω potentiometer
R_{11}	100 k Ω potentiometer
$D_{1,\dots,4}$	1n1419 diode
$U_{1,\dots,5}$	LM324 op. amp.

Table 1: The values of the electronic components employed in the construction of the tent map electronic circuit.

$$V_{out} = \frac{R_9 R_6}{R_8 R_7} V_{in} - \begin{cases} 0, & \text{for } V_{in} < \frac{R_1}{2R_2}, \\ \frac{R_9 R_5}{R_{10} R_4} \left(\frac{R_3 V_{in}}{R_1} - \frac{R_3}{2R_2} \right), & \text{for } V_{in} \geq \frac{R_1}{2R_2}, \end{cases} \quad (3)$$

where V_{in} and V_{out} are the input and output voltages of the tent map electronic circuit, respectively. It is worth noting that the switching block shown in Fig. 3 is realized through the **b** node,

$$V_b = \begin{cases} 0, & \text{for } V_{in} < \frac{R_1}{2R_2}, \\ \frac{R_5}{R_4} \left(\frac{R_3 V_{in}}{R_1} - \frac{R_3}{2R_2} \right), & \text{for } V_{in} \geq \frac{R_1}{2R_2}. \end{cases} \quad (4)$$

Thus, Eq. (3) is equivalent to Eq. (2) for the values of the components given in Table 1, and replacing V_{in} and V_{out} for x_n and x_{n+1} , respectively. In fact, this set of values is not unique because Eq. (3) contains several parameters. Thus, a circuit designer has the freedom to choose the particular components that satisfy other design constraints in a particular application. Despite of parasitic reactance, finite bandwidth of active components, and other experimental perturbations, the presented electronic circuit displays closely the behavior of the mathematical model given by Eq. (2). We implemented this design on a printed circuit board (PCB) manufactured in our laboratory. In the experimental circuit we used the LM324 operational amplifiers supplied with a power source at $\pm 15V$ and soldered directly to the PCB without a socket. The voltage V_{dc} was supplied by a variable dc supply with an output range of 0 – 15V. In order to have an iterative operation, see Fig. 2, this circuit considered a microcontroller PIC16F877A of Microchip, and a D/A converter DAC0800 of National Semiconductors with a processing time of 100 μs between voltage samples. Obviously, there are different ways to perform this iterative operation, but this is a matter that depends of the designer and the application.

The value of the bifurcation parameter μ can be fixed at certain values by simply adjusting the potentiometers R_5 and R_6 located in the operational amplifiers U_2 and U_3 . The relationship between the resistors R_5 and R_6 with the value of μ is given by equation (5), i.e., $\mu = R_5/2k\Omega = R_6/1k\Omega$.

$$V_{out} = \begin{cases} \frac{R_6}{1k\Omega} V_{in}, & \text{for } V_{in} < \frac{1}{2}, \\ \frac{R_5}{2k\Omega} \left(1 - \left(2 - \frac{2R_6}{R_5} \right) \right), & \text{for } V_{in} \geq \frac{1}{2}. \end{cases} \quad (5)$$

In order to explore the full range of the dynamics accessible to this circuit, we experimented with different values of R_5 and R_6 . These resistors were adjusted in the closed interval [1 k Ω , 4 k Ω]. Then μ was varied to obtain the bifurcation diagram shown in Fig. 5. In this figure, fixed points, periodic oscillations, period-doubling cascade and chaos can be clearly seen. From Fig. 5, it can be seen that the circuit exhibits the entire range of behaviors of the tent map. In fact, our experimental results of the dynamics of this circuit are found to be in good agreement with the theoretical values. Figure 6 (a) shows a time series of the output voltage for $\mu = 2$. In our measurements, each experimental time series contained 650 points collected for

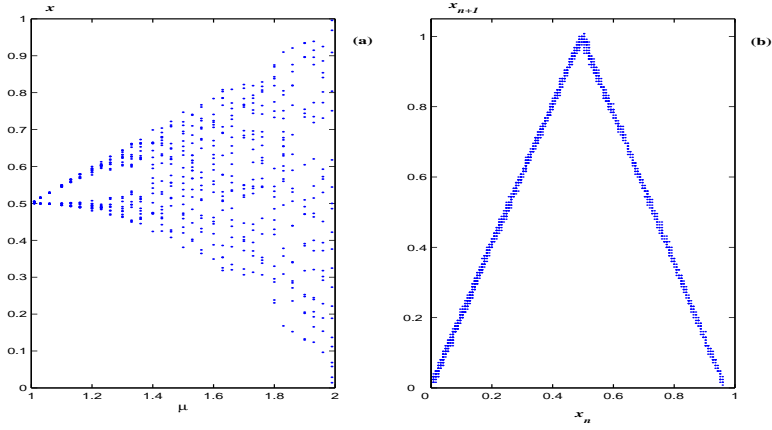


Fig. 5: Experimental bifurcation diagram for the tent map.

different values of the bifurcation parameter μ . Figure 6 (b) shows the histogram of the noise calculated over the 650 points. The noise time series r_n was estimated by the following equation

$$r_n = x_{n+1} - f(x_n), \quad (6)$$

where x_n and x_{n+1} are the experimental data of the tent map circuit, and $f(\cdot)$ is given by equation (2).

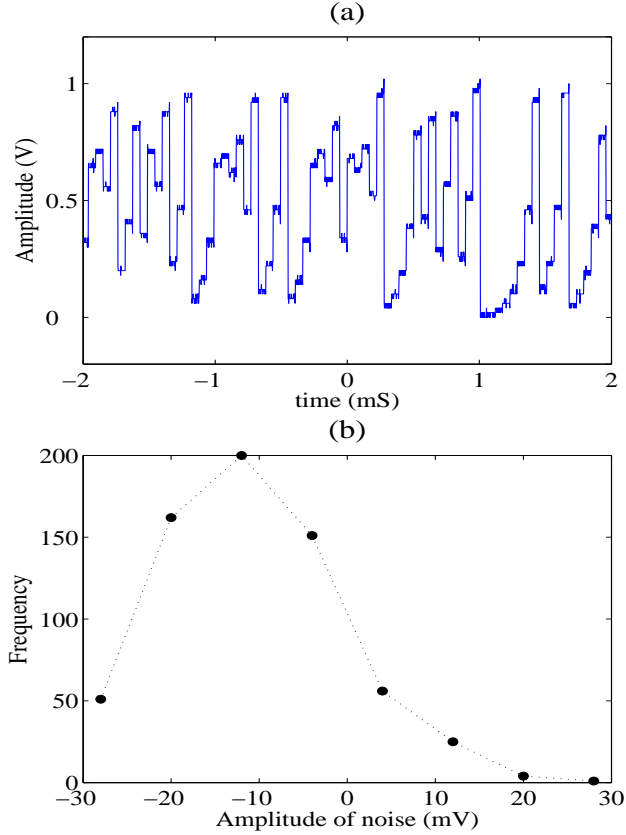


Fig. 6: (a) The time series with chaotic dynamics generated by the tent map for $\mu = 2$. (b) The histogram of the noise estimated by means of equation (6).

3 Conclusion

A very simple tent map electronic circuit has been presented here and its implementation using only analog components as operational amplifiers, diodes, and resistors was also provided. Therefore, it can be assembled even by students at the level of an undergraduate laboratory. Its experimental behavior was tested and compared with the numerical behavior given by the tent map difference equation. The circuit that replicates the whole known range of behaviors of the tent map has been determined. The employed techniques are simple and the approach can be extended to other types of maps such as the piecewise linear or piecewise smooth maps. Such circuit realizations have many potential applications, for example: random number generation, frequency hopping, ranging, and spread-spectrum communications. Finally, we notice that this design can be manufactured in just one chip because the final electronic circuit contains only semiconductors and passive components.

Acknowledgements

This work was supported by FAI-UASLP 2007 under contract C07-FAI-11-38.74 and also partially through the CONACyT project 46980.

References

- [1] May RM. *Simple mathematical models with very complicated dynamics*. Nature **261**, 459-467 (1976).
- [2] Li C. *A new method of determining chaos-parameter-region for the tent map*. Chaos, Solitons and Fractals 2004; 21: 863-867.
- [3] Billings L, Bollt EM. *Probability density functions of some skew tent maps*. Chaos, Solitons and Fractals 2001; 12: 365-376.
- [4] Huang W. *On complete chaotic maps with tent-map-like structures*. Chaos, Solitons and Fractals 2005; 24: 287-299.
- [5] Elaydi SN. *Discrete Chaos* (Chapman & Hall/CRC, Boca Raton, 2000).
- [6] Hasler M, Maistrenko YL, *Digital communications using chaos and nonlinear dynamics*. IEEE Trans. Circuits Syst. I: Fundam Theory Appl. **44**(10), 856-866 (1997).
- [7] Murali K, Sinha S, Ditto WL. *Realization of the fundamental NOR gate using a chaotic circuit*. Phys. Rev. E **68**, 016205 (2003).
- [8] Tanaka H, Sato S, Nakajima K. *Integrated circuits of map chaos generators*. Analog Integrated Circuits and Signal Processing **25**, 329-335 (2000).
- [9] Suneel M. *Electronic circuit realization of the logistic map*. Sadhana **31**(Part 1), 69-78 (2006).
- [10] Blakely JN, Eskridge MB, Corron NJ. *A simple Lorenz circuit and its radio frequency implementation*. Chaos **17**, 023112 (2007).